RSC Advances

ROYAL SOCIETY OF CHEMISTRY

www.rsc.org/advances

Journal Name

RSCPublishing

COMMUNICATION

Novel Poly-pyridyl Ruthenium Complexes with Bis- and Tris-tetrazolate Mono-dentate Ligands for Dye Sensitized Solar Cells†

Cite this: DOI: 10.1039/x0xx00000x

Tharallah A. Shoker [a] and Tarek H. Ghaddar [a]*

Received ooth January 2012,
Accepted ooth January 2012

DOI: 10.1039/x0xx00000x

www.rsc.org/

We report on a new family of ruthenium poly-pyridyl complexes that bears bis- and tris-tetrazolate mono-dentate ligands along with their spectroscopical, electrochemical, and theoretical characterization. Dye-sensitized solar cells with these complexes show good conversion efficiencies with comparable open circuit voltages to that of N719 without the use of any additives, due to their retarded electron-recombination processes.

In the past two decades high interest in the dye sensitized solar cell (DSSC) research area has been immense due to the DSSC's low cost of fabrication and ease of production,[1] which makes it a good candidate for commercialization. Recently, DSSC's efficiencies of 12.3% have been attained using a zinc-porphyrin complex as a sensitizer along with a liquid electrolyte system,[2] and efficiencies of 15% for perovskite-based solid state DSSC's.[3] Up-to-date, the most commonly used dye is either the well-known N3 dye (N719 when in the di-anionic form) $[Ru(NCS)_2(dcbpy)_2]$ (dcbpy = 4,4'-dicarboxy-2,2'-bipyridine)[4] or the black dye $[Ru(NCS)_3(tctpy)]$ (tctpy = 4,4',4''-tricarboxy- 2,2':6',2''-terpyridine)[5] as very efficient sensitizers. However, designing metal based dyes that lack the thiocyanate ligand (SCN^-), which is considered from long-term chemical stability tests as the weakest part in most ruthenium-based dyes,[6, 7] is of great interest. In addition, red-shifting the absorption band of the sensitizer in the visible and near-IR region may have positive effects on DSSCs' efficiencies.
Recently, a new class of cyclometalated complexes that lack the SCN^- ligand and have better light harvesting properties than N719 has been introduced by different research groups.[6-17] The high interest in this class of ruthenium based dyes is due to their good long term stability and extended absorption in the visible region (down to 800 nm). Most of this class of dyes is based on either bi- or tridentate ligands that bear either pyrazolate, triazolate, oxyquinolate, phenyl or pyrimidinyl moieties.

In the present study, we report the design of Ru^{II} based dyes, **T133** through **T136**, that bear bis- or tris-tetrazolate monodentate ligands along with either two (dcbpy) or one (tctpy) moiety, respectively, Scheme 1 (see Scheme S1 in the Supporting Information for the synthetic strategy). The interesting features of these four dyes are in their chemical stability, ease of synthesis/purification and their photophysical and electrochemical properties. To our knowledge, there are no reports of ruthenium based sensitizers that bear such monodentate ligands in the literature. The four dyes were characterized by ^{1}H-NMR, APPI mass spectrometry, UV/vis, steady state and lifetime fluorescence measurements and electrochemistry.

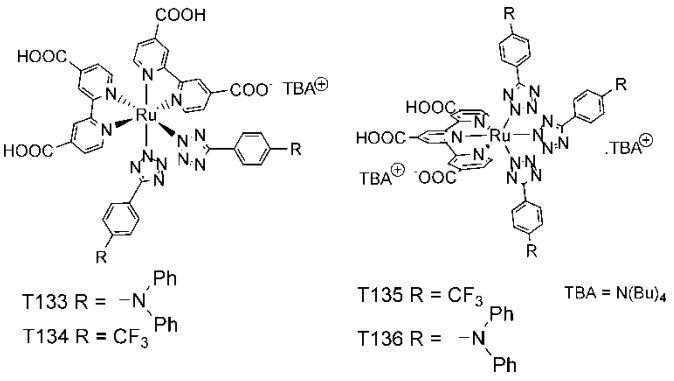

Scheme 1 Structures of the dyes T133 to T136

In the two dyes' classes (**T133-T134** and **T135-T136**) the tetrazolate ligand bares either an electron withdrawing trifluoromethylphenyl (TFMP) group or an electron rich triphenylamine (TPA) moiety, both of which tune the redox potential of the Ru^{II} center from 1.20 to 0.89 V vs. the normal

hydrogen electrode (NHE), Table 1. The presence of the electron rich TPA group would also red-shift the absorption maximum of the dye in the visible and near-IR region due to the increase in conjugation and electron donation ability. Whereas, the electron deficient TFMP group would raise the dye's redox potential when compared to the analogous TPA-based dye, which in turn ensures an efficient regeneration of the oxidized sensitizer by the iodide/triiodide electrolyte system upon electron injection.

The absorption and emission spectra of the four dyes in ethanol is depicted in Fig. 1. The first class of dyes (**T133-134**) shows an absorption in the visible region extending down to 750 nm (λ_{abs} = 513 nm and 508 nm with extinction coefficients ε = 9.3 and 9.9 x 10^3 M^{-1} cm^{-1} for **T133** and **T134**, respectively). The **T135** and **T136** absorption extends down to 820 nm with maxima at λ_{abs} = 566 nm and 572 nm and extinction coefficients ε = 7.9 and 6.8 x 10^3 M^{-1} cm^{-1}, respectively. The same trend was seen in the absorbance measurements done on 6 µm TiO_2 films dyed with the different dyes (see Fig. S4 in supporting information), suggesting that the amounts of the five different adsorbed dyes are similar. The lowest energy transitions are attributed to S_1 MLCT transitions inferred from TD-DFT calculations (see Table S1 and Fig. S2 in Supporting Information). The four dyes also show emission in the Near-IR region, Fig. 1, with intriguing longer lifetimes than most DSSC's dyes in the literature (see Fig. S3 in the Supporting Information). In aerated ethanol **T133** through **T136** show emission maxima at λ_{em} = 715, 705, 770 and 767 nm and emission lifetimes of τ_{em} = 70, 85, 120, 140 ns, respectively, Fig. 1 and Table 1. Such long emission lifetimes might positively add to the enhancement of electron injection efficiency.

Table 1 Spectroscopic and Electrochemical Data of the Dyes

	λ_{abs}, nm (ε, 10^4 M^{-1} cm^{-1})[a]	λ_{em}, nm (τ_{em}, ns)[b]	$E_{1/2}$, V vs NHE[c]	$E^*_{(ox)}$, V vs NHE
T133	311 (4.65), 380 (1.11), 513 (0.93)	715 (70)	1.35, 1.25, 1.10	-0.81
T134	311 (3.75), 380 (1.02), 508 (0.99)	705 (85)	1.20	-0.74
T135	337 (3.77), 385 (1.09), 566 (0.79)	770 (120)	1.00	-0.78
T136	333 (8.63), 388 (1.02), 572 (0.68)	767 (140)	1.35, 1.22, 0.89	-0.92
N719	306 (4.40), 379 (1.40), 525 (1.35)	755 (9)	1.08	-0.98

[a] Measured in ethanol. [b] Measured in aerated ethanol with λ_{ex} = 532 nm. [c] Measured in DMF with 0.1 M $TBAPF_6$.

The electrochemical properties of the different ruthenium complexes (**T133** through **T136**) were evaluated by differential pulse voltammetry in dimethylformamide (DMF), Fig. 2. (see also Fig. S1 in the Supporting Information). The $Ru^{II/III}$ redox potentials of the four dyes were measured to be $E_{1/2}$ = 1.10, 1.20, 1.00 and 0.89 vs NHE for **T133** through **T136**, respectively), Table 1. **T134** and **T135** showed only one redox peak between 0.2 and 1.5 V which is attributed to the oxidation/reduction of the $Ru^{II/III}$ center. Upon comparing the redox potentials of the four dyes shows that upon the introduction of a third tetrazolate ligand a shift of ~ 0.2 V is seen for **T135** and **T136** when compared to **T134** and **T133**, respectively. As expected, **T134** had the highest potential due to the electron donating effect of the TPA group on the ruthenium center. **T133** and **T136** show in addition to the ruthenium's redox potential two redox peaks in the scanned potential window which are attributed to the redox active TPA groups.

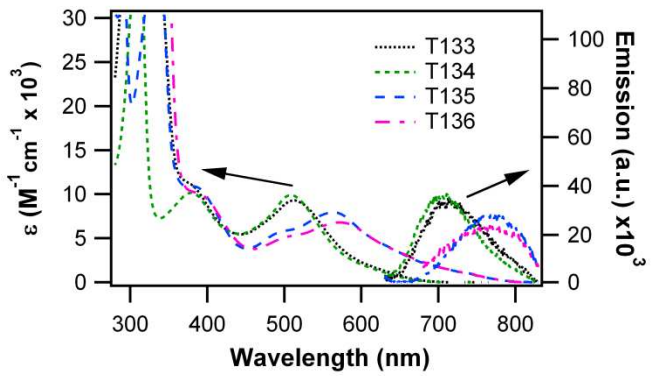

Fig. 1 Absorption and emission spectra (λ_{ex} = 532 nm) of **T133** (dotted-black), **T134** (dashed-green), **T135** (dashed-dotted-blue) and **T136** (dashed-dotted-dotted-violet) in ethanol.

The derived redox potentials of the dyes' excited states from both the $Ru^{II/III}$ redox potential and the optical energy gap (E_{0-0} was calculated from the intersection of the lowest energy MLCT band and the emission band) ranges between $E^*_{(ox)}$ = -0.74 and -0.92 V vs NHE. These values are higher than that of the TiO_2 conduction band edge (CB) (- 0.5 V vs. NHE), and thus upon photo excitation of these complexes fast and efficient electron injection into the TiO_2 CB is expected.

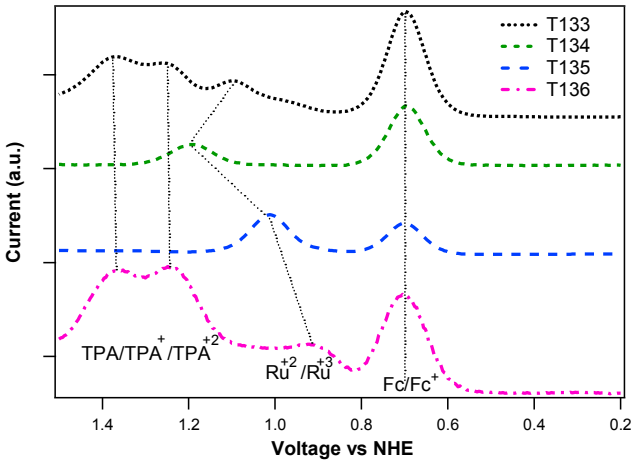

Fig. 2: Differential pulse voltammograms (0.1 M Bu_4NPF_6, DMF) for T133 to T136.

DSSCs employing a 12 µm thick TiO_2 layer plus a 4 µm scattering layer (300 nm) were fabricated using the four different dyes in addition to a DSSC employing the N719 dye for comparison. The TiO_2 films were stained by the respective dye solution (0.3 mM) in ethanol for 18 h without any additives. An electrolyte solution (EL1) made of 0.6 M 1,2-dimethyl-3-propylimidazolium iodide (MPII), 0.1 M guanadinium thiocyanate (GuNCS), 0.05 M LiI, 0.03 M I_2 and

0.5 M 4-*tert*-butylpyridine (TBP), in methoxypropanonitrile (MPN), was used in these studies. The photocurrent vs voltage (*IV*) responses of the above mentioned cells are shown in Fig. 3 and summarized in Table 2. The lower fill factors (*FF*) and open circuit voltages (V_{oc}) of the studied cells when compared to values in the literature are mainly due to the geometry of the cells studied (1 x 1 cm). The **T133** through **T136** based cells afforded good performances except for **T136**, with short-circuit photocurrents J_{sc} = 13.1, 12.0, 13.0 and 6.7 mA.cm^{-2}, V_{oc} = 620, 620, 622 and 495 mV, *FF* = 0.65, 0.67, 0.66 and 0.65 and efficiencies η = 5.3, 5.0, 5.3 and 2.2 %, respectively, under simulated AM1.5 G solar illumination at 100 mW.cm^{-2}. In the case of N719, the cell showed a slightly higher performance with J_{sc} = 14.6 mA.cm^{-2}, V_{oc} = 637 mV, *FF* = 0.67 and η = 6.2%.

The measured incident photon to electron conversion efficiency (IPCE) spectra of the **T133** through **T136** and N719 based cells are shown in Fig. 4. As can be seen, **T133** and **T134** show similar IPCE values to N719 but blue shifted by 20 and 25 nm, respectively, which is consistent with their UV/vis spectra. From the IPCE, integrated current and *IV* measurements one can conclude that **T133** and **T134** show similar electron injection and dye regeneration to N719.

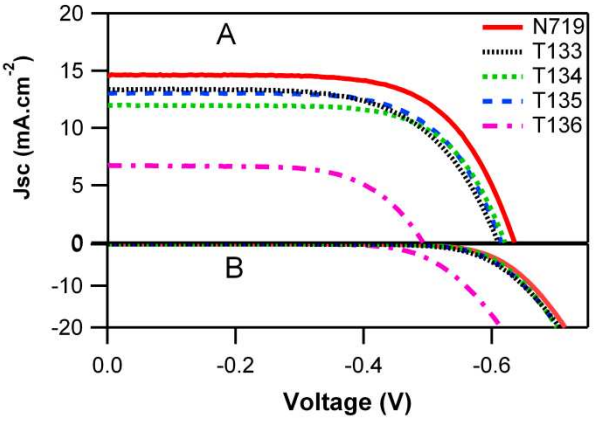

Fig. 3 (A) Photocurrent–voltage characteristics of DSSCs sensitized with dyes: N719 (solid-red) and **T133** (dotted-black), **T134** (dashed-green), **T135** (dashed-dotted-blue) and **T136** (dashed-dotted-dotted-violet) with electrolyte EL1. (B) Dark currents of the corresponding cells.

Table 2 DSSCs' Performance of **T133** through **T136** and **N719** Dyes

	J_{sc}, mA.cm^{-2}	V_{oc}, mV	*FF*	η (%)[a]
T133	13.1	620	0.65	5.3
T134	12.0	620	0.67	5.0
T135	13.0	622	0.66	5.3
T136	6.7	495	0.65	2.2
N719	14.6	637	0.67	6.2

[a] Measured under 100 mW.cm^{-2} simulated AM1.5 spectrum with an active area = 0.126 cm^2. Electrolyte EL1: 0.6 M DMPII, 0.05 M LiI, 0.5 M TBP, 0.1 M GuSCN and 0.03 M I_2 in MPN.

Moreover, the higher J_{sc} value shown by **T133** when compared to **T134** is mainly attributed to the former's better light absorption (5 nm red shift). As for **T135**, the IPCE spectrum shows lower IPCE% values but red shifted by ~ 20 nm when compared to N719. When using EL1 as the electrolyte system, **T136** shows much lower IPCE% values than N719 with a similar red shift as **T135** (this will be discussed at a later stage). The IPCE spectrum of **T135** highlights the better absorption nature of **T135** than N719 in the near-IR, however, the measured lower photo-current of **T135** could be attributed to its lower absorption extinction coefficient.

In order to understand the above mentioned results (lower efficiency of **T136** than N719), we performed electrochemical impedance spectroscopy (EIS) measurements on the five different assembled cells at V_{oc} under different light intensities. EIS spectra were analyzed using an established equivalent-circuit that interprets the different interfaces in a DSSC through a transmission line model.[18, 19] Fig. 5 shows a plot of the chemical capacitance values at the TiO_2/electrolyte interface (C_μ), for the different cells extracted from the EIS experiments, versus the corrected applied voltage $({}_nE_F - E_{F,redox})_{cor.}$, where ${}_nE_F$ is the electron quasi-Fermi energy level in the TiO_2 film and $E_{F,redox}$ is the electrolyte redox Fermi level, (the applied voltage is corrected for voltage drop due to the total series resistance,[20] R_s). The C_μ values for the five cells show an exponential behavior as a function of the corrected applied voltage, where this is due to the trap energy distribution below the conduction band edge.[21]

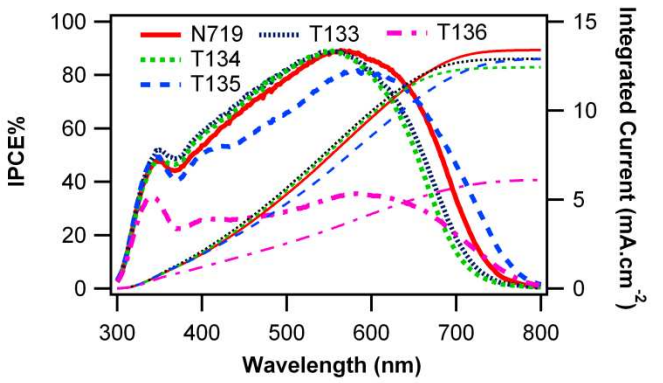

Fig. 4 IPCE% and integrated current spectra of N719 (solid-red) and **T133** (dotted-black), **T134** (dashed-green), **T135** (dashed-dotted-blue) and **T136** (dashed-dotted-dotted-violet) assembled cells with electrolyte EL1.

Considering that the five different cells have the same trap energy distribution (since the TiO_2 film is identical in all cells) and the same electrolyte solution is used in these cells, the observed shifts in the $({}_nE_F - E_{F,redox})_{cor.}$ towards higher or lower values could be attributed to an upward or downward shifts in the conduction band edge, respectively.[22, 23] The observed shifts $\Delta({}_nE_F - E_{F,redox})_{cor.}$ compared to N719 lies between +10 and -10 mV for the four tetrazolate based dyes, Fig. 5, which is within our data experimental errors. As such, we can assume that there is no significant shift in the conduction band edge in the five different cells. However, the plots of the charge recombination resistance at the TiO_2/electrolyte interface (R_{ct}) versus $({}_nE_F - E_{F,redox})_{cor.}$ show some differences between the five DSSCs, Fig. 6. DSSCs that incorporate **T133** through **T135** show slightly

smaller R_{ct} values than N719 (where a smaller R_{ct} value indicates faster electron recombination from the TiO_2 to the electrolyte solution or oxidized dye, and thus lower V_{oc} values). However, the **T136** based DSSC shows much smaller R_{ct} values than N719, which suggests fast electron recombination processes at the dyed TiO_2/electrolyte interface and in turn causes the low V_{oc} value of 495 mV. These results are also consistent with the dark currents measured for the respective cells, Fig. 3 B.

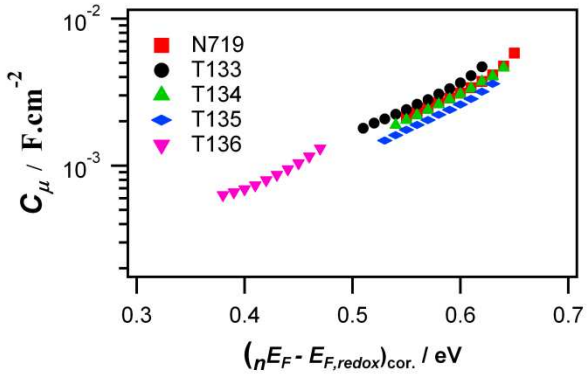

Fig. 5 Capacitance values obtained from EIS of N719 (square-red) and **T133** (circle-black), **T134** (triangle-green), **T135** (rhombus-blue) and **T136** (triangle-violet) assembled cells with electrolyte EL1.

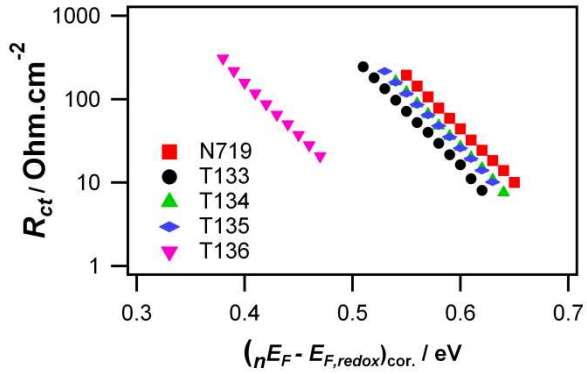

Fig. 6 Charge transfer resistance values obtained from EIS of N719 (square-red) and T133 (circle-black), T134 (triangle-green), T135 (rhombus-blue) and T136 (triangle-violet) assembled cells with electrolyte EL1.

Open circuit voltage decay (OCVD) experiments were conducted to probe the electron recombination processes. Fig. 7 shows the effective electron lifetime (τ_n) obtained from OCVD measurments,[24] in addition to the τ_n values derived from the EIS experiments (from EIS $\tau_n = R_{ct}.C_\mu$). Electron lifetimes obtained from the two different techniques (OCVD and EIS) are in good agreement. The τ_n values for the **T133** through **T135** based cells are only ~ 1.7 times shorter than that of N719. However, **T136**, and as inferred by all of the performed measurements, shows a much shorter τ_n than N719 by ~ 52 times.

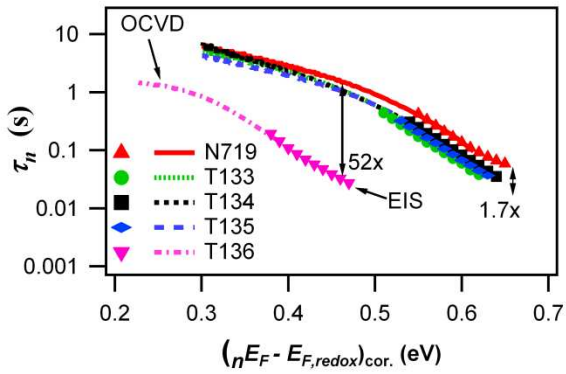

Fig. 7 Electron lifetimes obtained from OCVD and EIS of N719 (square-red) and **T133** (circle-black), **T134** (triangle-green), **T135** (rhombus-blue) and **T136** (triangle-violet) assembled cells with electrolyte EL1.

Therefore, the slight lower performance of **T133** to **T135** than N719 is due to the blue-shift in the absorption spectra of **T133** and **T134** and slightly faster electron recombination processes, whereas that of **T135** is due to the latter reason and its low absorption extinction coefficient. However, the much lower efficiency of **T136** when compared to **T133-T135** and N719 is mainly due to accelerated electron recombination processes. The accumulated electrons in the TiO_2 can either recombine with the oxidized dye upon electron injection or to the electrolyte system. The former mechanism becomes significant when the oxidized dye is not sufficiently regenerated by the electrolyte redox system.[25] In addition, the dye structure can have profound effects on the electron recombination processes, where it was shown by different research groups that depending on the molecular structure of the dye binding to iodine[26] or even iodide[27] can take place and affect the DSSC performance negatively or positively, respectively. In order to pinpoint the reason behind such increased electron recombination kinetics in the case of **T136**, we used a different electrolyte system (EL2: 2.0 M 1,3-dimethylimidazolium iodide (DMII), 0.1 M GuNCS, 0.05 M LiI, 0.03 M I_2 and 0.5 M TBP in MPN) that we and other groups[14] use with dyes that possess redox potentials below 1.0 eV vs NHE and might be inefficiently regenerated with electrolyte systems with low iodide concentrations such as in EL1. Indeed, with EL2 (compared to EL1) **T136** shows an increase in efficiency from 2.2 % to 5.3% with higher values of J_{sc} = 12.8 mA.cm^{-2} and V_{oc} = 630 mV than that with EL1, Fig. 8.

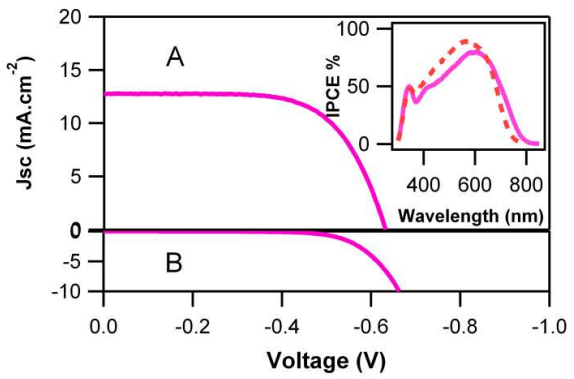

Fig. 8 (A) Photocurrent–voltage characteristics of **T136** DSSC with EL2 as the electrolyte system; (inset) IPCE spectra of N719 (dashed-red) and **T136** (solid-violet) using EL2. (B) Dark current of the corresponding **T136** cell.

In addition, **T136** shows a comparable electron lifetime to the other dyes when EL2 is used as the corresponding electrolyte, (see Fig. S5 in the Supporting Information). Therefore, it would be safe to conclude that in the case of **T136** the lower performance shown with EL1 than with EL2 might be due to an inefficiency in its regeneration by EL1. However, at this point one cannot be sure if this is due to **T136** lower redox potential than the other three dyes or to its different molecular structure when anchored on TiO_2.

Conclusions

In summary, we have successfully designed and synthesized a new class of ruthenium based dyes using bis- and tris-tetrazolate ligands that show interesting photophysical and electrochemical properties. Good DSSCs efficiencies were attained with these new dyes and will surely be improved in the near future, and the achievement of comparable efficiencies to the N719 cells is remarkable for this first new family of dyes. We are currently designing similar dyes with long aliphatic chains and increased conjugation. Using long aliphatic chains, on such more manipulative ligands than a thiocyanate is, would decrease electron recombination processes.[28, 29] Whereas extending the conjugation in these ligands might increase the absorption extinction coefficient and thus attain better light harvesting ability.

Acknowledgments

This work was supported by the University Research Board (URB) at the American University of Beirut (AUB) and the Lebanese National Council for Scientific Research (LNCSR).

Notes and references

[a] American University of Beirut PO Box: 11-0236, Beirut, Lebanon.

† Electronic Supplementary Information (ESI) available: [details of any supplementary information available should be included here]. See DOI: 10.1039/c000000x/

1. B. O'Regan and M. Grätzel, *Nature*, 1991, **353**, 737-740.
2. A. Yella, H.-W. Lee, H. N. Tsao, C. Yi, A. K. Chandiran, M. K. Nazeeruddin, E. W.-G. Diau, C.-Y. Yeh, S. M. Zakeeruddin and M. Grätzel, *Science*, 2011, **334**, 629-634.
3. J. Burschka, N. Pellet, S.-J. Moon, R. Humphry-Baker, P. Gao, M. K. Nazeeruddin and M. Grätzel, *Nature*, 2013, **499**, 316–319.
4. M. K. Nazeeruddin, F. De Angelis, S. Fantacci, A. Selloni, G. Viscardi, P. Liska, S. Ito, B. Takeru and M. Grätzel, *J. Am. Chem. Soc.*, 2005, **127**, 16835-16847.
5. M. K. Nazeeruddin, P. Pechy, T. Renouard, S. M. Zakeeruddin, R. Humphry-Baker, P. Comte, P. Liska, L. Cevey, E. Costa, V. Shklover, L. Spiccia, G. B. Deacon, C. A. Bignozzi and M. Grätzel, *J. Am. Chem. Soc.*, 2001, **123**, 1613-1624.
6. T. Bessho, E. Yoneda, J.-H. Yum, M. Guglielmi, I. Tavernelli, H. Imai, U. Rothlisberger, M. K. Nazeeruddin and M. Grätzel, *J. Am. Chem. Soc.*, 2009, **131**, 5930-5934.
7. M. Grätzel, *Acc. Chem. Res.*, 2009, **42**, 1788-1798.
8. T. Funaki, M. Yanagida, N. Onozawa-Komatsuzaki, K. Kasuga, Y. Kawanishi, M. Kurashige, K. Sayama and H. Sugihara, *Inorg. Chem. Commun.*, 2009, **12**, 842-845.
9. H. Kisserwan and T. H. Ghaddar, *Dalton Trans.*, 2011, **40**, 3877–3884.
10. K. C. D. Robson, B. D. Koivisto, A. Yella, B. Sporinova, M. K. Nazeeruddin, T. Baumgartner, M. Grätzel and C. P. Berlinguette, *Inorg. Chem.*, 2011, **50**, 5494-5508.
11. P. G. Bomben, K. C. D. Robson, B. D. Koivisto and C. P. Berlinguette, *Coord. Chem. Rev.*, 2012, **256**, 1438-1450.
12. K.-L. Wu, S.-T. Ho, C.-C. Chou, Y.-C. Chang, H.-A. Pan, Y. Chi and P.-T. Chou, *Angew. Chem. Int. Ed.*, 2012, **51**, 5642-5646.
13. C.-C. Chou, K.-L. Wu, Y. Chi, W.-P. Hu, S. J. Yu, G.-H. Lee, C.-L. Lin and P.-T. Chou, *Angew. Chem. Int. Ed.*, 2011, **50**, 2054-2058.
14. C.-W. Hsu, S.-T. Ho, K.-L. Wu, Y. Chi, S.-H. Liu and P.-T. Chou, *Energy Environ. Sci.*, 2012, **5**, 7549-7554.
15. T. Funaki, H. Funakoshi, O. Kitao, N. Onozawa-Komatsuzaki, K. Kasuga, K. Sayama and H. Sugihara, *Angew. Chem. Int. Ed.*, 2012, **51**, 7528-7531.
16. H. C. Zhao, J. P. Harney, Y.-T. Huang, J.-H. Yum, M. K. Nazeeruddin, M. Grätzel, M.-K. Tsai and Rochford, *J. Inorg. Chem.*, 2012, **51**, 51.
17. B. Schulze□, D. G. Brown, K. C. D. Robson, C. Friebe□, M. Jäger□, E. Birckner, C. P. Berlinguette and U. S. Schubert□*Chem. Eur. J.*, 2013, **19**, 1521–3765.
18. Q. Wang, S. Ito, M. Grätzel, F. Fabregat-Santiago, I. n. Mora-Seró, J. Bisquert, T. Bessho and H. Imai, *J. Phys. Chem. B*, 2006, **110**, 25210-25221.
19. F. Fabregat-Santiago, G. Garcia-Belmonte, I. Mora-Sero and J. Bisquert, *PCCP*, 2011, **13**, 9083-9118.
20. T. Stergiopoulos, M. Konstantakou and P. Falaras, *RSC Advances*, 2013, **3**, 15014-15021.
21. J. Bisquert, *PCCP*, 2003, **5**, 5360-5364.
22. V. Gónzalez-Pedro, X. Xu, I. n. Mora-Seró and J. Bisquert, *ACS Nano*, 2010, **4**, 5783-5790.
23. E. Guillén, L. M. Peter and J. A. Anta, *J. Phys. Chem. C*, 2011, **115**, 22622-22632.
24. A. Zaban, M. Greenshtein and J. Bisquert, *Chemphyschem*, 2003, **4**, 859-864.
25. K. C. D. Robson, K. Hu, G. J. Meyer and C. P. Berlinguette, *J. Am. Chem. Soc.*, 2013, **135**, 1961-1971.
26. X. Li, A. Reynal, P. Barnes, R. Humphry-Baker, S. M. Zakeeruddin, F. De Angelis and B. C. O'Regan, *PCCP*, 2012, **14**, 15421-15428.
27. J. Jeon, W. A. Goddard and H. Kim, *J. Am. Chem. Soc.*, 2013, **135**, 2431-2434.
28. L. Schmidt-Mende, J. E. Kroeze, J. R. Durrant, M. K. Nazeeruddin and M. Grätzel, *Nano Lett.*, 2005, **5**, 1315-1320.
29. S. M. Zakeeruddin, M. K. Nazeeruddin, R. Humphry-Baker, P. Pechy, P. Quagliotto, C. Barolo, G. Viscardi and M. Grätzel, *Langmuir*, 2002, **18**, 952-954.

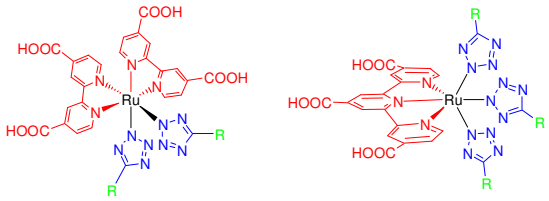

New Ru^{II} complexes bearing bis- and tris-tetrazolate ligands, and their application as efficient sensitizers in Dye-sensitized Solar Cells are presented.